New Insights into Water Splitting at Mesoporous α-Fe$_2$O$_3$ Films: A Study by Modulated Transmittance and Impedance Spectroscopies

Charles Y. Cummings,[†] Frank Marken,[†] Laurence M. Peter,*[,†] K. G. Upul Wijayantha,[‡] and Asif A. Tahir[‡]

[†]Department of Chemistry, University of Bath, Claverton Down, Bath BA2 7AY, United Kingdom
[‡]Department of Chemistry, Loughborough University, Loughborough LE11 3TU, United Kingdom

S *Supporting Information*

ABSTRACT: Thin mesoporous films of α-Fe$_2$O$_3$ have been prepared on conducting glass substrates using layer-by-layer self-assembly of ca. 4 nm hydrous oxide nanoparticles followed by calcining. The electrodes were used to study the oxygen evolution reaction (OER) in the dark and under illumination using in situ potential-modulated absorption spectroscopy (PMAS) and light-modulated absorption spectroscopy (LMAS) combined with impedance spectroscopy. Formation of surface-bound higher-valent iron species (or "surface trapped holes") was deduced from the PMAS spectra measured in the OER onset region.

Similar LMAS spectra were obtained at more negative potentials in the onset region of photoelectrochemical OER, indicating involvement of the same intermediates. The impedance response of the mesoporous α-Fe$_2$O$_3$ electrodes exhibits characteristic transmission line behavior that is attributed to slow hopping of holes, probably between surface iron species. Frequency-resolved PMAS and LMAS measurements revealed slow relaxation behavior that can be related to the impedance response and that indicates that the lifetime of the intermediates (or trapped holes) involved in the OER is remarkably long.
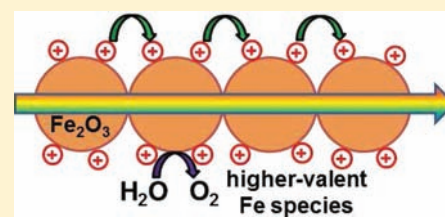
INTRODUCTION

α-Fe$_2$O$_3$ (hematite) has been investigated extensively as a potential photoanode material for water splitting cells.[1−6] Although its band gap (∼2.0 eV) is suitable for harvesting visible light and its valence band is low enough in energy for holes to oxidize water, an external bias is needed to raise the free energy of electrons in the conduction band sufficiently to drive the hydrogen evolution reaction at the counter-electrode to split water. The necessary external voltage bias can be provided by a solar cell in a tandem cell configuration.[7] Performance limitations imposed by high doping and short hole diffusion lengths in hematite films have been addressed by nanostructuring the electrode to enhance the chances of holes reaching the oxide/electrolyte interface.[8,9] However, surface and bulk recombination losses still limit performance, and to make progress toward the ultimate goal of efficient water splitting, it is essential to understand these processes.

Recent work in our laboratory[10,11] confirms that the light-driven oxygen evolution reaction (OER) at hematite involves very slow electron transfer, as suggested originally by Dare-Edwards et al.[1] At the same time, surface recombination of electrons and holes shifts the photocurrent onset away from the flatband potential, degrading the efficiency of the water splitting process. It has been shown that this loss process can be minimized by treatment of the surface of the hematite layer with a cobalt solution,[4] but we have shown that the improvement arises from suppression of surface recombination rather than from catalysis of the electron transfer process, which remains remarkably slow, implying substantial buildup of intermediate species.[11] These intermediates can be considered either as surface trapped holes or as higher-valent iron species formed at the surface by hole capture.

Recent studies of hematite films using pulsed laser excitation have identified a long-lived transient absorption that has been attributed to surface trapped holes.[12,13] The reported decay time of this transient absorption (seconds) is very similar to the slow decay seen in photocurrent transients.[11] The competition between electron transfer and recombination that determines the transient photocurrent response and the external quantum efficiency has been characterized quantitatively in our laboratories using photoelectrochemical impedance spectroscopy (PEIS) and intensity-modulated photocurrent spectroscopy (IMPS).[10,11] These experiments showed that electron transfer and surface recombination processes at hematite photoelectrodes are both unusually slow, with estimates of surface intermediate concentrations approaching monolayer levels at solar intensities.[10,11] The present study used in situ absorbance spectroscopy to detect and compare surface intermediate species formed during the OER in the dark and under illumination. The required sensitivity was obtained either by modulating the electrode potential in the case of the dark OER (potential-modulated absorbance spectroscopy: PMAS) or by modulating the intensity of illumination in the case of the light-driven OER (light-modulated absorbance spectroscopy: LMAS). In both cases, well-resolved normalized absorbance spectra were obtained that suggest that the "surface trapped holes"[12,13] are in fact long-lived higher-valent Fe species formed as intermediates in the OER. A parallel study of the system

using impedance spectroscopy led to a clear understanding of the frequency dependence of the modulated absorbance response and allowed deconvolution of the total impedance. Analysis of the transmission line behavior observed in the high frequency part of the impedance showed that hole transport is slow and probably occurs via hopping between adjacent surface Fe sites. The long lifetimes of the "trapped hole" states derived from these measurements are similar to the values obtained in our previous work on compact hematite layers by photoelectrochemical impedance spectroscopy (PEIS)[10] and by intensity-modulated photocurrent spectroscopy (IMPS).[11]

■ EXPERIMENTAL METHODS

NaOH, FeCl$_3$, HClO$_4$, and carboxymethylcellulose (sodium salt) were obtained in analytical reagent grade from Sigma-Aldrich. Solutions were prepared with deionized and filtered water from a Thermo Scientific water purification system (Barnstead Nanopure) with 18.2 MΩ cm resistivity. Films of mesoporous iron oxide were fabricated by a layer-by-layer technique developed in our laboratory.[14,15,16] A stable colloidal solution of hydrous iron oxide nanoparticles (ca. 4 nm in diameter by TEM and SAXS[16]) was prepared by hydrolysis of ferric chloride in boiling water followed by dialysis against aqueous HClO$_4$ (pH 3.5).[17] A conducting glass slide (fluorine-doped tin oxide coating: TEC 8. Libbey Owens Ford) was immersed into the 2 mM colloidal solution for 1 min to bind a monolayer of oxide particles. After being rinsed and dried, the film was immersed for 1 min into a solution containing 1.5% w/w carboxymethylcellulose (sodium salt). Rinsing and drying completed one deposition cycle. This process was repeated until the desired number of layers was obtained. The multilayer films were calcined in a tube furnace at 500 °C in air for 30 min to remove the organic components, leaving an orange-brown mesoporous iron oxide (hematite) film. The electrode area exposed to the electrolyte was 1 cm^2. Figure 1 illustrates the effect of the number of layers
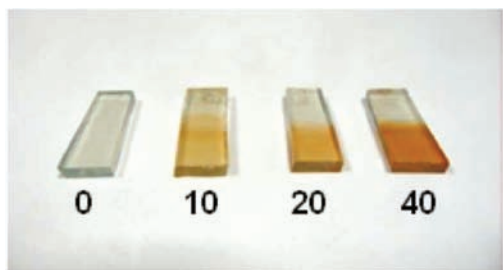

Figure 1. Mesoporous α-Fe$_2$O$_3$ films prepared by layer-by-layer dip coating of conducting glass. The numbers shown indicate the number of dip cycles.

deposited on the color of the films. Further details of film characterization have been given elsewhere.[15,16]

The electrolyte used in all of the measurements was 0.1 M NaOH. A MicroAutolab III potentiostat system (EcoChemie, NL) was used for cyclic voltammetry, and a low noise battery-powered potentiostat was used for PMAS and LMAS. The optical cell incorporated a platinum wire counter electrode and a KCl saturated calomel reference electrode (SCE, Radiometer). Impedance measurements were made using a Solartron 1250 frequency response analyzer with a Solartron 1286 electrochemical interface. PMAS measurements were performed using monochromatic light provided by a Xe lamp light source and monochromator (Bentham Instruments). Transmitted light was detected with a silicon photodiode connected to a lock-in amplifier (Stanford Research SR 830) via a low noise current amplifier. The sinusoidal potential modulation (100 mV p−p, 35.4 mV rms) was provided by the lock-in amplifier. Spectra were recorded at a frequency of 2.7 Hz and at 90° phase shift with respect to the sinusoidal potential modulation to eliminate the small background signal arising from electroreflectance effects from the FTO substrate. LMAS measure-

ments were performed using a tungsten optical fiber illuminator and a monochromator (Bentham Instruments). The modulated illumination (80% depth) was provided by a 370 nm light emitting diode (LED: Thorlabs) coupled via a LED driver (Thorlabs) to the signal output of the lock-in amplifier. A 2 mm GG400 nm filter (Schott) was used in front of the silicon photodiode detector to minimize light throughput from the UV LED. The frequency response of the PMAS and LMAS signals at constant wavelength (460 nm) was measured using the Solartron 1250 frequency-response analyzer.

■ THEORETICAL BASIS

If a surface species is formed by reversible oxidation of a surface site, for example:

$$Fe(III)_{surf} \rightleftharpoons Fe(IV)_{surf} + e^- \tag{1}$$
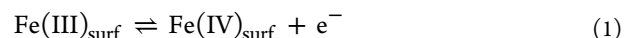
then modulation of the potential close to the standard potential of the redox couple leads to a corresponding periodic change in the number densities (concentrations) of oxidized and reduced species (Δn_O, Δn_R − referred to the geometric area) that depends on the Faradaic charge passed, that is, on the integral of the Faradaic component of the total ac current.

$$\tilde{Q}_F = zq\Delta n_O = -zq\Delta n_R = \int j_F(\omega t)dt \tag{2}$$

where z is the number of electrons transferred and q is the elementary charge. The corresponding normalized change in absorbance depends on the difference in (wavelength dependent) optical absorption cross sections, $\sigma_O(\lambda)$ and $\sigma_R(\lambda)$, of the two species.[18,19]

$$\frac{\Delta T}{T} = \Delta n[\sigma_O(\lambda) - \sigma_R(\lambda)]$$

$$= \frac{\tilde{Q}_F}{zq}[\sigma_O(\lambda) - \sigma_R(\lambda)] \tag{3}$$

To derive the frequency dependence of the PMAS response, it is necessary to consider the total impedance of the system, which in the present case is a mesoporous film. The theory of impedance of finite porous electrodes has been reviewed and generalized by Bisquert.[20] Electron transport and electron transfer can be represented in a transmission line model as shown in Figure 2a (the additional series resistance, R_{ser}, arising mainly from the FTO substrate and contacts, is not shown). The model describes charge transport in the electrode material as well as the transfer and storage of charge at the electrode/electrolyte interface. r_{trans} is the distributed transport resistance, r_{ct} is the charge transfer resistance, and C_{surf} is the capacitance of the α-Fe$_2$O$_3$/electrolyte interface. We assume that the dominant contribution to the capacitance comes from pseudocapacitance associated with the surface redox reaction. The particle size is sufficiently small (4 nm) that band bending is likely to be negligible, which means that the contribution of the space charge capacitance can be neglected, and also the redox pseudocapacitance is expected to be larger than the double layer capacitance. Because the α-Fe$_2$O$_3$ film is mesoporous, it is reasonable to assume that electron (or hole) transport is driven by diffusion, because charges in the particles will be shielded effectively by the electrolyte so that any macroscopic electrical field will be negligible. At low frequencies, the transmission line reduces to the parallel RC circuit shown in Figure 2b, which is in series with the resistance of the FTO substrate electrode. The time constant $R_{ct}C$ corresponding to the discharge of the pseudocapacitance

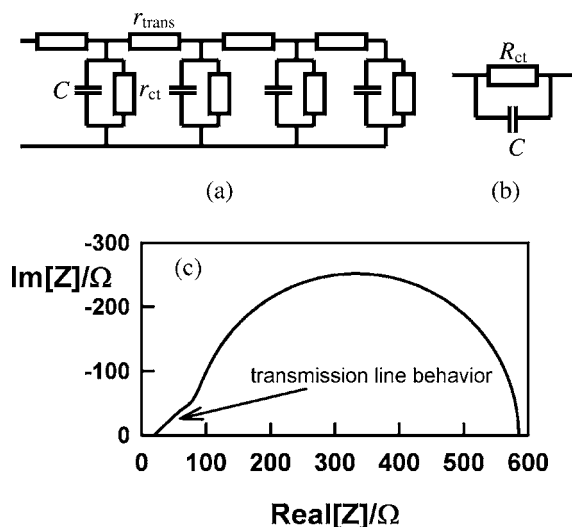**Figure 2.** (a) Finite transmission line representing the impedance of the porous α-Fe$_2$O$_3$ electrodes. (b) Equivalent circuit in the low frequency limit. The additional series resistance is not shown in either circuit. (c) Typical impedance response for the transmission line circuit including a series resistance. Note the linear region at high frequencies, which is characteristic of transmission line behavior.

through the Faradaic resistance effectively represents the lifetime of the surface-bound redox species.

As shown in the Supporting Information, the periodic component of the charge stored by the pseudocapacitance can be expressed in terms of a complex capacitance C_c:

$$\tilde{Q}_F = C_c \tilde{V} \qquad (4)$$

where $\tilde{V}$ is the voltage modulation. An example of the calculated frequency dependence of the modulated charge stored in the pseudocapacitance is shown in Figure 3. In the
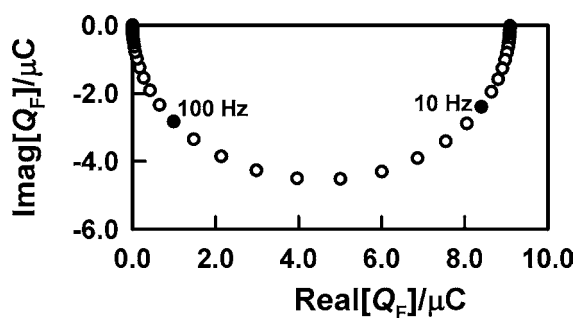

Figure 3. Frequency dependence of the modulated charge Q_F on the pseudocapacitance in Figure 2b calculated for a series resistance of 50 Ω, $R_{ct} = 500$ Ω, $C = 10^{-4}$ F, and a modulation amplitude of 100 mV. The potential-modulated absorbance response should exhibit an identical frequency response.

case where $R_{ser} < R_{ct}$, the characteristic time constant corresponding to the minimum of the semicircular response is determined by the series combination of the series resistance and the capacitance. In the case where $R_{ct} < R_{ser}$, the time constant is determined by the decay of charge through the Faradaic resistance; i.e., it is a measure of the lifetime of the surface-bound species. Because the modulation of the absorbance is linearly dependent on the modulation of stored charge, the PMAS response should mirror the charge response, showing the same characteristic relaxation frequency. As

mentioned above, in the case where $R_{ser} < R_{ct}$, the relaxation frequency does not reflect the "lifetime" of the surface intermediate; this must be obtained from analysis of the electrode impedance as shown below.

■ RESULTS AND DISCUSSION

OER in the Dark. A typical cyclic voltammogram of the mesoporous α-Fe$_2$O$_3$ films is shown in Figure 4. The quasi-

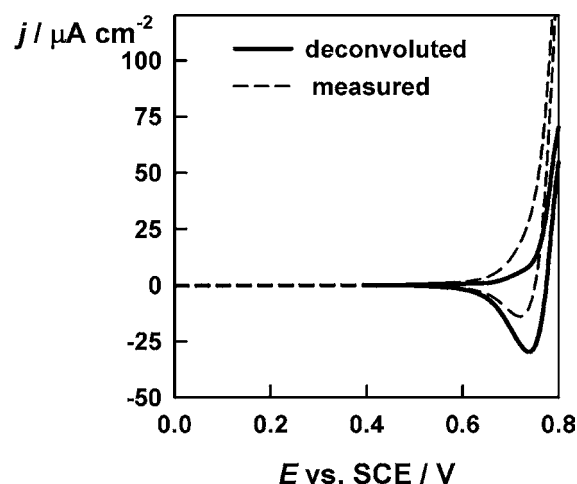**Figure 4.** (− − −) Cyclic voltammogram of a 20 layer film. Sweep rate 100 mV s^{-1}. (−) Current after correction for steady-state OER current and substrate charging current.

reversible behavior at the onset of oxygen evolution suggests the formation of a higher valent Fe species. In previous work, it has been shown that this surface species (tentatively identified as Fe(IV)) is active in the oxidation of glucose.[16] The figure also shows the deconvoluted voltammogram obtained by subtraction of the steady-state OER current (which was fitted to a Tafel slope of 93 mV/decade) and of the background charging current from the FTO substrate. The anodic and cathodic charge associated with the quasi-reversible couple is of the order of 25 μC cm^{-2} for an anodic limit of 0.8 V.

PMAS spectra recorded at different dc potentials in the range 0.65−0.85 V vs SCE are illustrated in Figure 5 for a 20 layer film. The spectra exhibit two well-defined peaks (460 and 560 nm) and a shoulder at around 770 nm. Similar spectra with two clear peaks were measured for the 10 layer film, whereas the peaks, although still evident, were not so pronounced as for the 40 layer film. The PMAS response increases with voltage, peaking at 0.725 V before falling at higher dc voltages. The shapes of the spectra appear to be independent of dc potential, suggesting that only one surface-bound redox couple is involved.

PMAS measures the difference in absorbance brought about by potential modulation (cf., eq 3). The well-defined spectra in Figure 5 correspond to a decrease in transmittance when the potential is made more positive, that is, when oxidation takes place. Impedance measurements (see below) showed that the pseudocapacitance associated with surface oxidation is of the order of 0.5 mF cm^{-2} (geometric) at 0.7 V for a 20 layer film. It follows that the modulated charge (rms) in the PMS experiments is ca. 20 μC cm^{-2}, corresponding to $\Delta n_O \approx 10^{14}$ cm^{-2} (geometric). This is consistent with the charge under the reduction peak in the voltammogram shown Figure 1 (ca. 25 μC cm^{-2}). Assuming a nanoparticle packing fraction = 0.5, the
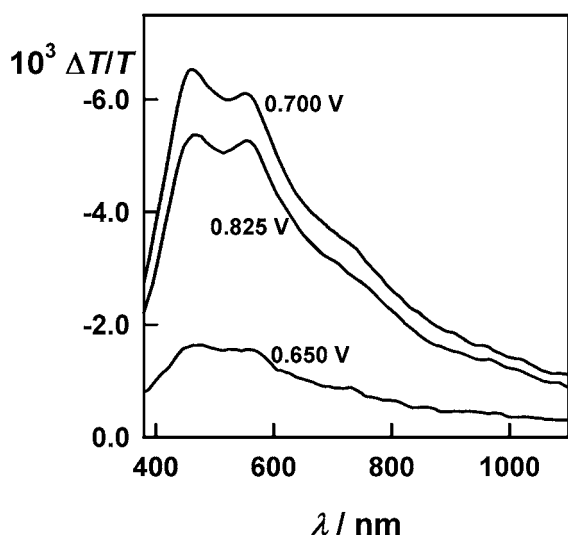
1230

dx.doi.org/10.1021/ja209530s | *J. Am. Chem. Soc.* 2012, 134, 1228−1234

Figure 5. PMAS spectra for a 20 layer mesoporous α-Fe$_2$O$_3$ layer measured at the dc potentials shown. Modulation 2.7 Hz, 100 mV peak−peak.

Figure 6. Voltammogram of 40 layer α-Fe$_2$O$_3$ film under chopped monochromatic illumination. Sweep rate 10 mV s^{-1}. Illumination 365 nm, 10 mW cm^{-2}. The apparent variation in the height of the current spikes is an artifact arising from the digital signal sampling.

internal surface area of the 20 layer film (ignoring necking during sintering) should be ∼30 cm^2. It follows that the surface concentration of oxidized species (or "surface trapped holes") is ∼4 × 10^{12} cm^{-2}, that is, around 1% of a monolayer. The $\Delta T/T$ value at the peak in the PMAS spectrum (460 nm) measured at 0.7 V can be used to calculate the difference in absorption cross sections as 6 × 10^{-17} cm^2, corresponding to a difference in molar absorption coefficient $\varepsilon = 3.6 \times 10^4$ dm^3 mol^{-1} cm^{-1}.

The PMAS spectra and molar absorption coefficients of surface species can be compared to known absorption spectra of higher valent Fe species. The absorption spectra reported for Fe(IV), Fe(V), and Fe(VI) species in solution in the region 400−700 nm have been reviewed recently by Sharma and Virender.[21] Fe(IV) shows a broad peak at 420 nm ($\varepsilon = 1200$ dm^3 mol^{-1} cm^{-1}). Fe(VI) has a broad peak at 510 nm ($\varepsilon = 1100$ dm^3 mol^{-1} cm^{-1}). Fe(V) has a main peak at 400 nm ($\varepsilon = 900$ dm^3 mol^{-1} cm^{-1}) and a second peak at 500 nm ($\varepsilon = 650$ dm^3 mol^{-1} cm^{-1}). Clearly, none of these solution species correspond to the observed PMAS spectra. The most striking difference is that the molar absorption coefficient of the surface species appears to be more than an order of magnitude higher than that of the ferrate ions. Other possibilities that can be considered are low spin and high spin iron peroxo species, which show charge transfer bands in the visible at around 550 nm,[22,23] but these complexes (with organic ligands) also have absorption coefficients in the region of 10^3 dm^3 mol^{-1} cm^{-1}, that is, lower than those estimated for the surface-bound species detected by PMAS.

Light-Driven OER. The photoelectrochemical OER takes place at much less positive potentials than the dark OER as can be seen from the voltammogram shown in Figure 6, which was recorded in the potential range where LMAS spectra were measured. The anodic photocurrents observed with the mesoporous α-Fe$_2$O$_3$ films used in the present study are considerably smaller than those measured with films of similar thickness prepared in our laboratories by aerosol-assisted CVD[10,11] (possibly as a consequence of the absence of a space charge region), and the substantial losses due to surface recombination are evident in the spiked response. The photocurrent onset potential could not be determined for
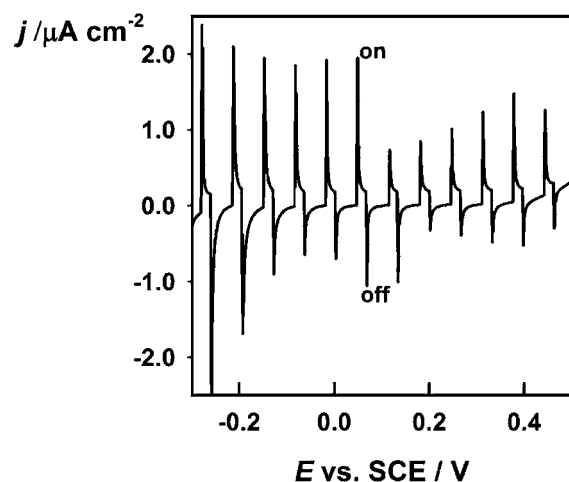
these mesoporous films because reduction takes place at more negative potentials.[16]

Light-driven OER at α-Fe$_2$O$_3$ involves holes that are formed by excitation of electrons from the valence band to the conduction band. By contrast, holes required for the OER in the dark must be created by another mechanism. In the case of bulk thin films of highly doped α-Fe$_2$O$_3$ under inversion conditions, holes can be created at the oxide/electrolyte interface via electron tunneling from the valence band to the conduction band across the narrow space charge region. This mechanism seems unlikely for the mesoporous films in which band bending is expected to be minimal. An alternative mechanism involves oxidation of surface Fe sites at the substrate/Fe$_2$O$_3$ contact followed by progressive oxidation of the internal surface of the mesoporous layer by hole hopping (or equivalent electron hopping) between adjacent surface sites. This process is analogous to the hole hopping process that takes place between dye molecules adsorbed on mesoporous TiO$_2$.[24,25] In both light-driven and dark OER, we may expect to form higher valent iron species at the surface. In the case of the photoelectrochemical OER on α-Fe$_2$O$_3$, our previous work suggests that a substantial concentration of "trapped holes" will accumulate at the surface because OER involves very slow electron transfer. This conclusion is supported by recent work by Pendlebury et al.,[12,13] who observed a long-lived transient absorbance following pulsed laser excitation of α-Fe$_2$O$_3$ electrodes. The spectra reported by Pendlebury et al., which are broadly similar to those in Figure 7, were attributed to "surface trapped holes". In the present study, LMAS was used to investigate optical changes brought about by illumination of mesoporous α-Fe$_2$O$_3$ electrodes with a near UV LED. The electrode potentials were chosen to lie in the region where photocurrents corresponding to photoelectrochemical OER are observed. Figure 7 illustrates the LMAS spectra obtained. Although the spectra were noisier than the PMAS spectra, their structure is very similar (the data in Figure 7 have been smoothed to allow better comparison with Figure 5). The LMAS response is nearly 2 orders of magnitude lower than in the PMAS spectra, reflecting the fact that the internal quantum efficiency for the photoelectrochemical OER is small, because
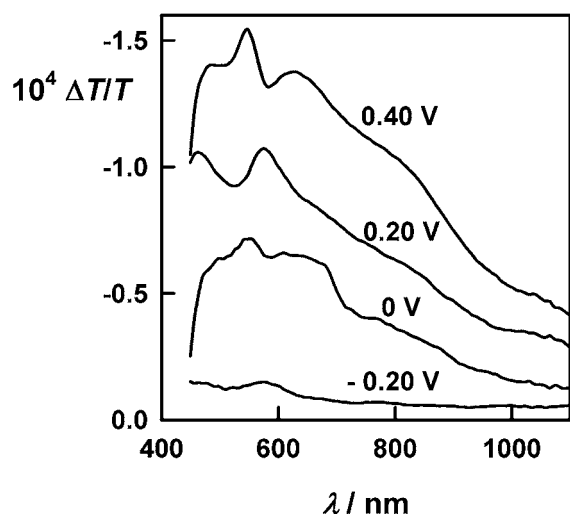
Figure 7. LMAS spectra recorded for a 20 layer α-Fe$_2$O$_3$ film at the potentials (vs SCE) shown.

the majority of holes formed by illumination are lost by recombination.

As we have shown elsewhere,[10,11] the photoinduced concentration of intermediates (trapped holes) at the surface of α-Fe$_2$O$_3$ electrodes is determined by the hole flux into the surface and the first-order rate constants for recombination and interfacial charge transfer. The fact that the intermediates can be detected spectroscopically indicates that the rate constants are small (for bulk thin films of the order of 10 s^{-1} or less[10,11]). In the present case, the surface concentration of intermediate states (referred to the internal surface area) can be estimated by comparing the magnitude of the largest LMAS and PMAS responses to be $\sim$10^{11} cm^{-2}. Because the measured photo-current density ($\sim$1 μA cm^{-2}: cf., Figure 6) corresponds to a flux of holes into the internal surface equal to 2×10^{11} cm^{-2} s^{-1}, the lifetime of the intermediate should be of the order of 0.5 s, which is consistent with the photocurrent decay seen in the transient photocurrent response as a consequence of surface recombination. This calculation highlights the very long lifetimes of the "surface trapped hole" intermediates involved in the photoelectrochemical OER.

Frequency Dependence of the PMAS and LMAS Responses. It was found that the PMAS and LMAS responses of the α-Fe$_2$O$_3$ films are attenuated at high frequencies, so that a low frequency (2.7 Hz) was used for all of the measurements of spectra. To understand the frequency dependence of the PMAS response of the α-Fe$_2$O$_3$ films, impedance measurements were carried out (in the dark) in the potential range where PMAS spectra were recorded. Figure 8 illustrates a typical impedance response, which exhibits transmission line behavior in the high frequency region of the complex plane plot. The fit to the data to the model shown in Figure 2 is excellent, as can be seen more easily in the phase angle part of the Bode plot.

The variation of R_{ct}, R_{trans}, and C with electrode potential was recorded for 10, 20, and 40 layer α-Fe$_2$O$_3$ films. Figure 9 illustrates the trends with the example of the 40 layer film. It can be seen that the time constant $R_{ct}C$ corresponding to the "lifetime" of the oxidized Fe states decreases from 0.1 s to 10 ms as the potential is increased from 0.7 to 0.8 V, reflecting the increasing rate of electron transfer in the OER.
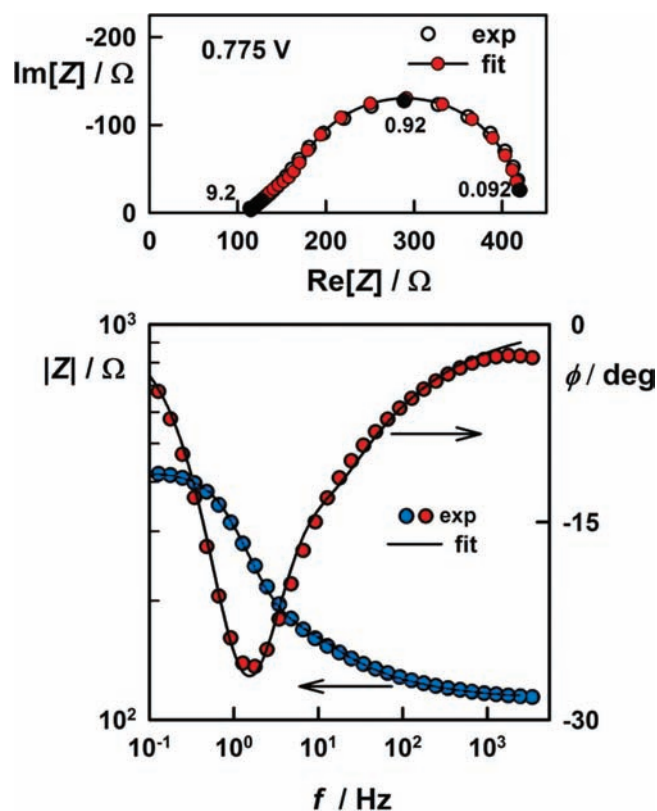

Figure 8. Impedance of 40 layer α-Fe$_2$O$_3$ film measured in the dark at 0.775 V vs SCE showing the fit of the data to the transmission line model (cf., Figure 2a). The frequencies in Hz are labeled on the complex plane plot. Fit values R_{ct} = 275 Ω, R_{trans} = 161 Ω, C = 0.68 mF.
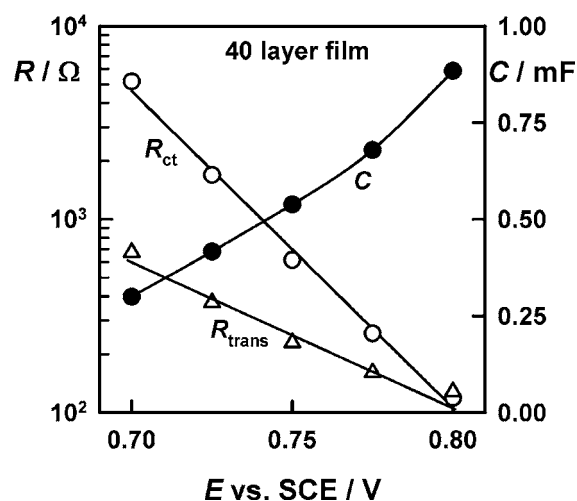

Figure 9. Potential dependence of transport resistance, R_{trans}, charge transfer resistance, R_{ct}, and capacitance, C, for a 40 layer α-Fe$_2$O$_3$ film. Values derived from the fitting to the equivalent circuit are shown in Figure 2a with inclusion of the series resistance.

The transmission line behavior seen in the impedance response suggests slow transport of charge in the mesoporous α-Fe$_2$O$_3$ film. Hole transport in α-Fe$_2$O$_3$ is known to be slow and to depend strongly on direction in the crystal lattice. In a recent theoretical study, Iordanova et al.[26] have modeled electron and hole transport in α-Fe$_2$O$_3$ using Marcus theory and obtained hole mobilities of 3.6×10^{-7} and 1.7×10^{-4} cm^2

V^{-1} s^{-1} for transport in the (001) plane and along the [001] axis, respectively. The transport resistance measured by impedance spectroscopy is related to the hole concentration by

$$R_{tr} = \frac{d_{film}}{\sigma} = \frac{d_{film}}{qp\mu_p} \qquad (5)$$

where d_{film} is the film thickness and the conductivity σ is determined by the product of the hole mobility, μ_p, and the hole concentration p. The decrease in R_{trans} observed in the semilogarithmic plot in Figure 9 can be interpreted as an exponential increase of hole concentration with potential. If we take the lower value of mobility and consider a 80 nm film with $R_{tr} = 100\ \Omega$ (cf., Figure 9) at 0.8 V, the free hole concentration would be 1.4×10^{18} cm^{-3}, corresponding to charge of 1.8 μC cm^{-2} (geometric). This is an order of magnitude lower than the charge (ca. 20 μC cm^{-2}) estimated from the pseudocapacitance. If the mean mobility is higher, the hole concentration will be correspondingly lower still. We therefore consider the possibility that hole transport in the mesoporous film is even slower than in the bulk because holes are localized at the surface of the α-Fe_2O_3 nanoparticles, with transport occurring via a hole hopping mechanism involving the higher valent Fe species observed in the PMAS spectra. To examine this model semiquantitatively, we need to establish a correspondence between the electrical and optical properties of the film. In other words, we need to relate the impedance of the films to the frequency-dependent PMAS response. Figure 10 shows that
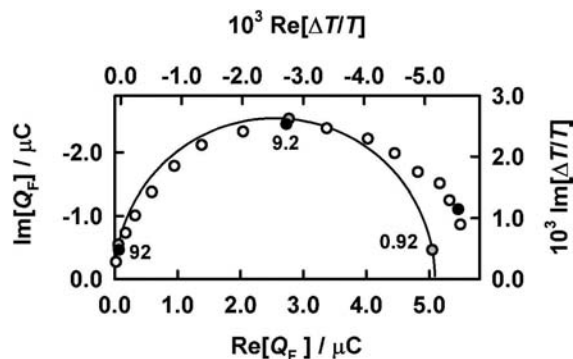

Figure 10. Comparison of frequency dependence of the PMAS response of a 20 layer mesoporous α-Fe_2O_3 film at 0.775 V vs SCE with the rms modulated charge calculated from the complex capacitance obtained using values of R_{ct}, C, and R_{ser} derived from the impedance analysis. Line fit. Frequencies in Hz as shown: black experimental $\Delta T/T$, gray fit.

there is indeed a one to one correspondence between the frequency dependence of the modulated transmission and the modulated charge on the pseudocapacitance, validating the model given in the theoretical section (in the present case, the frequency attenuation arises predominantly from the combination of series resistance and pseudocapacitance).

As discussed above, the surface concentration of higher valent iron species ("surface trapped holes") in the potential range where a large PMAS response is observed is estimated to be of the order of 4×10^{12} cm^{-2}, which corresponds to a volume concentration of around 10^{19} cm^{-3}. Therefore, if we interpret the transport resistance as arising from hopping of surface trapped holes between sites, the mobility would be an order of magnitude lower than the values for the bulk, that is,

ca. 4×10^{-8} cm^2 V^{-1} s^{-1}, which corresponds to a diffusion coefficient of 10^{-9} cm^2 s^{-1}. This low diffusion coefficient is consistent with thermally activated electron transfer between adjacent Fe sites on the surface. A crude estimate based on an average hopping distance of 0.5 nm and an attempt frequency of 10^{13} s^{-1} gives an activation energy of around 0.4 eV, which corresponds to the depth of the hole trap.

The LMAS response is also attenuated at high frequencies, as can be seen from the results in Figure 11. The relaxation in this
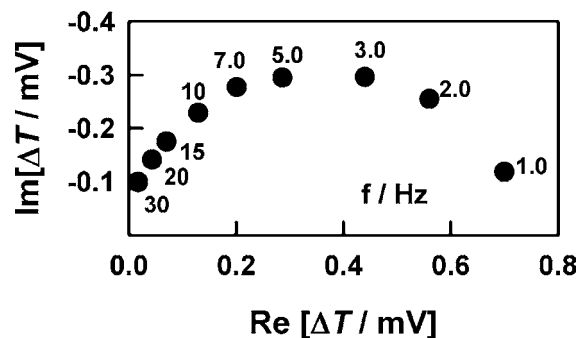

Figure 11. Frequency response of the LMAS response at 600 nm, 0.40 V vs SCE. Frequencies in Hz as shown.

case can be related to the corresponding slow relaxation seen in the transient photocurrent (cf., Figure 6). The lifetime of the surface trapped hole intermediate derived from the frequency of the maximum in Figure 11 is about 50 ms.

We have recently reported the determination of rate constants for hole transfer and recombination at compact α-Fe_2O_3 electrodes using intensity modulated photocurrent spectroscopy (IMPS).[11] The results were fitted using a model in which holes are trapped at surface states and can then either react to form oxygen or recombine with conduction band electrons. The characteristic relaxation frequency in this case corresponds to the sum of the rate constants for hole transfer, k_{tr}, and recombination, k_{rec}, and the lifetime is the reciprocal of the sum of $k_{tr} + k_{rec}$. The time constant derived from Figure 11 is consistent with the values measured by IMPS on compact α-Fe_2O_3 films, and we can therefore conclude that we are seeing the decay of the higher valent Fe species ("trapped holes") as they are consumed either by the OER or by capture of electrons from the conduction band of the Fe_2O_3. It follows that the LMAS and PMAS spectra provide a spectroscopic footprint of the "trapped hole" intermediate in the OER.

CONCLUSIONS

The combination of spectroscopic and impedance techniques has given a deeper insight into the mechanism and kinetics of oxygen evolution at α-Fe_2O_3. The same species is detected in potential-modulated and light-modulated transmittance measurements, suggesting that the mechanisms of oxygen evolution involve the same intermediate in the dark and under illumination. The slow relaxation seen in light-modulated experiments and in impedance measurements confirms the existence of a kinetic bottleneck in the OER at α-Fe_2O_3. The chemical identity of the intermediate detected by modulated spectroscopy has not been established, but if we consider it as a "surface-trapped hole", higher order reactions are required for the four-electron oxidation of water. An elementary step involving 4-holes can be discounted, so that it is reasonable to assume that hole capture leads to Fe states with valencies

higher than +4. As we have suggested elsewhere, the OER could involve adjacent surface sites corresponding nominally to Fe(V) or to Fe(IV) and Fe(VI). This would mean more than one hole must be captured at each site before oxygen evolution can proceed. In this context, the mobility of surface holes becomes important, and the low hole mobilities inferred from the impedance analysis suggest that the sluggishness of the OER may be due, at least in part, to slow surface diffusion, that is, to deep trapping of holes in addition to the activation energy associated with O−O bond rupture.

■ ASSOCIATED CONTENT

Ⓢ Supporting Information

Derivation of the complex capacitance of the circuit in Figure 2. This material is available free of charge via the Internet at http://pubs.acs.org.

■ AUTHOR INFORMATION

Corresponding Author

l.m.peter@bath.ac.uk

■ ACKNOWLEDGMENTS

■ REFERENCES

(1) Dare-Edwards, M. P.; Goodenough, J. B.; Hamnett, A.; Trevellick, P. R. *J. Chem. Soc., Faraday Trans. 1* **1983**, *79*, 2027.

(2) Sivula, K. L. F. F.; Grätzel, M. *ChemSusChem* **2011**, *4*, 432.

(3) Bjorksten, U.; Moser, J.; Grätzel, M. *Chem. Mater.* **1994**, *6*, 858.

(4) Kay, A.; Cesar, I.; Grätzel, M. *J. Am. Chem. Soc.* **2006**, *128*, 15714.

(5) Kennedy, J. H.; Anderman, M. *J. Electrochem. Soc.* **1983**, *130*, 848.

(6) Quinn, R. K.; Nasby, R. D.; Baughman, R. J. *Mater. Res. Bull.* **1976**, *11*, 1011.

(7) Grätzel, M. *Nature* **2001**, *414*, 338.

(8) Brillet, J.; Grätzel, M.; Sivula, K. *Nano Lett.* **2010**, *10*, 4155.

(9) Cesar, I.; Sivula, K.; Kay, A.; Zboril, R.; Grätzel, M. *J. Phys. Chem. C.* **2009**, *113*, 772.

(10) Wijayantha, K. G. U.; Saremi-Yarahmadi, S.; Peter, L. M. *Phys. Chem. Chem. Phys.* **2011**, *13*, 5264.

(11) Peter, L. M.; Wijayantha, K. G. U.; Tahir, A. A. *Faraday Discuss.* **2012**, DOI: 10:1039/C1FD00079A.

(12) Pendlebury, S. R.; Barroso, M.; Cowan, A. J.; Sivula, K.; Tang, J. W.; Grätzel, M.; Klug, D.; Durrant, J. R. *Chem. Commun.* **2011**, *47*, 716.

(13) Cowan, A. J.; Barnett, C. J.; Pendlebury, S. R.; Barroso, M.; Sivula, K.; Grätzel, M.; Durrant, J. R.; Klug, D. R. *J. Am. Chem. Soc.* **2011**, *133*, 10134.

(14) McKenzie, K. J.; Marken, F. *Pure Appl. Chem.* **2001**, *73*, 1885.

(15) McKenzie, K. J.; Marken, F.; Hyde, M.; Compton, R. G. *New J. Chem.* **2002**, *26*, 625.

(16) Cummings, C. Y.; Bonne, M. J.; Edler, K. J.; Helton, M.; McKee, A.; Marken, F. *Electrochem. Commun.* **2008**, *10*, 1773.

(17) Mulvaney, P.; Cooper, R.; Grieser, F.; Meisel, D. *Langmuir* **1988**, *4*, 1206.

(18) Hutton, R. S.; Kalaji, M.; Peter, L. M. *J. Electroanal. Chem.* **1989**, *270*, 429.

(19) Kalaji, M.; Peter, L. M. *J. Chem. Soc., Faraday Trans.* **1991**, *87*, 853.

(20) Bisquert, J. *Phys. Chem. Chem. Phys.* **2000**, *2*, 4185.

(21) Sharma, V. K. *J. Environ. Manage.* **2011**, *92*, 1051.

(22) Eugster, N.; Jensen, H.; Fermin, D. J.; Girault, H. H. *J. Electroanal. Chem.* **2003**, *560*, 143.

(23) Roelfes, G.; Vrajmasu, V.; Chen, K.; Ho, R. Y. N.; Rohde, J. U.; Zondervan, C.; la Crois, R. M.; Schudde, E. P.; Lutz, M.; Spek, A. L.; Hage, R.; Feringa, B. L.; Munck, E.; Que, L. *Inorg. Chem.* **2003**, *42*, 2639.

(24) Fattori, A.; Peter, L. M.; McCall, K. L.; Robertson, N.; Marken, F. *J. Solid State Electrochem.* **2010**, *14*, 1929.

(25) Fattori, A.; Peter, L. M.; Wang, H. X.; Miura, H.; Marken, F. *J. Phys. Chem. C* **2010**, *114*, 11822.

(26) Iordanova, N.; Dupuis, M.; Rosso, K. M. *J. Chem. Phys.* **2005**, *122*, 144305.